Proceedings of IMECE04
2004 ASME International Mechanical Engineering Congress
November 13-19, 2004, Anaheim, CA USA

IMECE2004-61850

FINITE ELEMENT ESTIMATION OF THE RESIDUAL STRESSES IN ROLLER-STRAIGHTENED RAIL

Brandon Talamini
Jeff Gordon
US Department of Transportation
John A. Volpe National Transportation Systems Center
Cambridge, MA 02142 USA

A. Benjamin Perlman
Department of Mechanical Engineering
Tufts University
Medford, MA 02155 USA

ABSTRACT

The purpose of this paper is to develop models to accurately predict the residual stresses due to the roller straightening of railroad rails. Several aspects of residual stress creation in rail due to roller straightening are addressed. The effect of the characteristics of the loads applied by the roller-straightener on the stress profile is examined. In addition, the analysis attempts to discern the relative influence of bending and contact on the residual stresses. The last goal is to determine how the heat treatment of rail alters the predicted roller-straightening residual stress field.

The loads for the simulation are estimated from available data. To identify the most credible values, a baseline loading case is defined and modeled. These straightening loads are parameterized by considering alternative loading scenarios. Residual stresses and deformations are calculated using these loads.

To separate the effects of bending and contact on the residual stress induced by the roller loads, each credible load case is analyzed with two models. One is a 2-dimensional generalized plane strain (GPS) model that accounts only for the flexural stresses. The other is a fully 3-dimensional analysis that includes roll-on-rail contact to make estimates of the true residual stress field. Comparison of the residual stress results from both models reveals the relative influence of local roll-rail contact and bending on the final profile.

Comparison of the 2- and 3-dimensional residual stress results reveals that the magnitude of the contact loads is a decisive influence on the stress field, even in portions of the rail web located far from the contact interface. Therefore, it is critical to obtain accurate estimates of the straightening loads to make accurate roller straightening residual stress estimates.

Heat treatment of the rail prior to roller straightening primarily affects the longitudinal residual stress in the web, causing a positive shift in the stress values.

INTRODUCTION

Residual stresses contained in railroad rails are known to affect the growth rate of fatigue cracks that lead to rail failure. In particular, longitudinal tensile stress in the head accelerates the growth rate of transverse flaws.

Rails develop residual stresses during manufacturing and in service. Measurement of these stresses is difficult and costly. Analytical estimates of the residual stress field due to service have been previously made [1]. The residual stresses due to the heat treatment portion of the rail manufacturing process have also been computed [2]. However, it is not known how the initial stress distribution due to the roller-straightening manufacturing process affects these calculations. This paper presents a method for determining these manufacturing stresses.

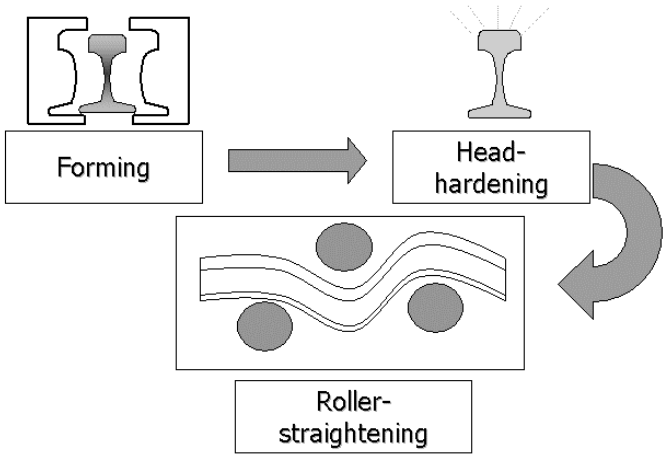

Figure 1. Schematic of the steps of the rail manufacturing process.

Currently, rails manufactured in the United States are made in three steps: forming by hot rolling, heat treatment, and roller straightening (see Figure 1). First, steel blooms are shaped into rails. Since this operation occurs above the austenitizing temperature of the rail, recrystallization occurs quickly, and any stresses induced during this process are quickly relieved [3]. Residual stresses in rails leaving the mill are introduced during the heat treatment and the roller straightening processes.

The differential cooling rate due to the geometry of the rail and the quenching operation causes the rails to acquire curvature. The rails need to be straightened before they can be shipped and installed. This is most commonly done in a cold rolling operation called *roller straightening*. It is during this stage that most of the residual stress is developed due to the large amounts of associated plastic strain.

In the United States, roller straightening is done with a series of 9 rolls: 4 fixed driven upper rolls, and 5 lower idler rolls that are vertically adjustable (see Fig. 2) [3]. The rail is fed through the roll stands, which are arranged to bend the rail alternately upwards and downwards. The rail is deformed plastically under the rolls, and after passing through all of the stands, the curvature is completely removed.

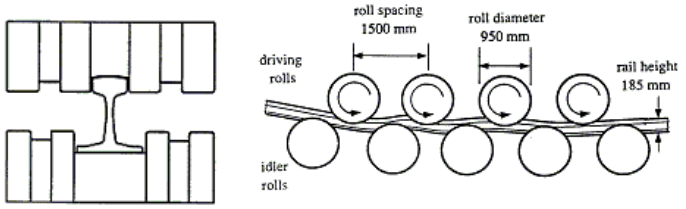

Figure 2. Schematic of roller straightening (from reference [3]).

STRATEGY

This paper addresses several aspects of residual stress creation in rail due to roller straightening. The effect of the characteristics of the loads applied by the roller-straightener on the stress profile is examined. In addition, the analysis attempts to discern the relative influence of bending and contact on the residual stresses. The last goal is to determine how the heat treatment of rail alters the predicted roller-straightening residual stress field.

Analytical estimates and experimental measurements of the residual stresses in rail have been made previously [3-6, 8]. The results are contradictory and suggest no clear trend. Roller straightening is a nonlinear, time-dependent structural problem that is strongly influenced by the load application history. Temperature dependent, elastic and inelastic material properties of the rail steel are needed to properly describe the total manufacturing process. There is no reliable source for this mechanical data. In addition, no carefully designed measurement of the forces at every roll stand in the roller-straightener has been published.

In this study, linear kinematic hardening behavior is assumed for the analysis. Properties typical for North American rail steel are used.

The loads for the simulation are estimated from available data. To identify the most credible values, a baseline loading case is defined and modeled. These straightening loads are parameterized by considering alternative loading scenarios. Residual stresses and deformations are calculated using these loads.

To separate the effects of bending and contact on the residual stress induced by the roller loads, each credible load case is analyzed with two models. One is a 2-dimensional generalized plane strain (GPS) model that accounts only for the flexural stresses. The other is a fully 3-dimensional analysis that includes roll-on-rail contact to make estimates of the true residual stress field. Comparison of the residual stress results from both models reveals the relative influence of local roll-rail contact and bending on the final profile.

Simulations including initial heat treatment stresses for the most credible load cases are compared to results that exclude this feature. To ascertain the effect of this part of the manufacturing process on the roller straightening stresses, a heat treatment stress field previously calculated for a typical North American head-hardening operation is used for the comparison [2].

The 132RE rail section is used for all of the calculations. This section is commonly found in North American rail networks. It is also the North American section that is the most geometrically similar to the International Union of Railways' UIC60 section, which is prevalent in rail systems abroad. This choice facilitates comparisons to data gathered worldwide.

All calculations are performed with the commercial finite element code ABAQUS/Standard, version 6.4-1 [7].

STRAIGHTENING LOAD SCENARIOS

In the absence of reliable force measurements made at every roll stand, the loading within the roller straightener must be estimated. The approach adopted here is to define a baseline load case using the best

available data, and then to vary the values in subsequent cases to determine the sensitivity of the residual stresses to loading.

The only published experimental data on roller-straightening operating conditions available to the authors is in a report from the International Union of Railways' Office of Research and Experiments (ORE) [8]. This document reports measurements of the displacement settings for the adjustable rolls and of the forces at 3 of the 9 roll stands for the straightening of UIC60 rails. It is necessary to determine the loads at the other rolls to conduct a simulation of the process.

Four loading cases are defined and compared in this paper. The baseline loading scenario is adapted from a roller straightening analysis made by Wineman [3]. This analysis interpreted the measurements from [8] as a set of roller loads and bending moments. To scale these bending moments to sections other than the test rail, the moments are reported as dimensionless numbers that are normalized to the magnitude of the bending moment that initiates yielding in the outer fiber of the rail. Figure 3 is a diagram of how the normalized bending moments are scaled. The moment magnitudes for load case 1 are scaled to a 132RE rail section on the left axis of Fig. 3. For example, the bending moment at the third roll is given as 1.42 M_y, where M_y is the product of yield strength and the section modulus of the rail. To define the contact loads for the baseline case in this paper, the reaction forces at each roll stand are back-calculated from the bending moment ratios using the equilibrium equations of statics.

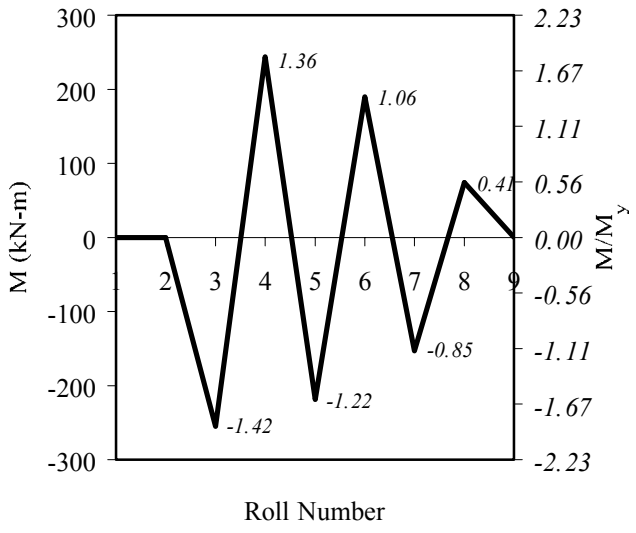

Figure 3 Moment diagram using the moment ratio information from Wineman [3]. The left axis shows the values scaled to a 132RE section assuming a yield stress of 483 MPa.

In addition to the normalized bending moment values in reference [3], there are also estimated values of the reaction forces at the roll stands. The values agree with the force measurements from reference [8] at the rolls where measurements were made. However, these forces do not agree with the forces that are back-calculated from the bending moments in Fig. 3, but they instead appear to be scaled up from these by a constant factor (approximately 15%). The second load case is defined by scaling up the loads from case 1 by this factor. In essence, load case 2 matches the available force measurements from the ORE study.

The third case is aimed at finding the low-end of the straightening loads range. For this case, the baseline loads were reduced by 15%.

The fourth load case is derived from the roll displacement measurements in reference [8]. A beam element model was constructed of the rail, and the measured roll displacements were applied as boundary conditions (the fixed rolls were set to have no displacement). The reaction force generated at each roll represents the net contact force applied by the roller–straightener at that location. These loads are larger than any of the other estimates. For more detail on this calculation, refer to Talamini [9]. The procedure of this calculation is similar to the work in [3], however, the results do not agree.

The four load cases are summarized in tables 1 and 2 below. Table 1 contains the maximum bending moments applied to the rail. Positive bending moments place the rail head in compression. Table 2 contains the net contact forces applied at each roll. Positive forces are impressed on the base of the rail, while negative forces are applied to the rail head.

Table 1. Bending moment data for every load case.

	Roll Number								
	1	2	3	4	5	6	7	8	9
Case 1									
MR	0	0	-1.42	1.36	-1.22	1.06	-0.85	0.41	0
M (kN-	0	0	-255	244	-219	190	-153	74	0
Case 2									
MR	0	0	-1.67	1.60	-1.44	1.25	-1.0	0.48	0
M (kN-	0	0	-300	287	-258	224	-180	87	0
Case 3									
MR	0	0	-1.21	1.16	-1.04	0.90	-0.72	0.35	0
M (kN-	0	0	-217	207	-186	162	-130	63	0
Case 4									
MR	0	0	-1.9	1.93	-1.93	1.13	-1.84	0.32	0
M (kN-	0	0	-338	344	-345	202	-328	57	0

Table 2. Roll contact force data for every load case.

	Roll Number								
	1	2	3	4	5	6	7	8	9
Case 1 Force (kN)	0	-340	1005	-1282	1162	-1002	760	-377	74
Case 2 Force (kN)	0	-400	1182	-1508	1367	-1179	894	-444	87
Case 3 Force (kN)	0	-289	854	-1090	988	-852	646	-320	63
Case 4 Force (kN)	0	-451	1361	-1829	1648	-1435	1219	-648	135

Two primary criteria are used to evaluate the load cases: straightness and the maximum depth of the elastic-plastic interface. These criteria are explained below.

Straightness – This criterion is simple: the curvature of the rail during roller straightening can be determined from a finite element model of the process. Load cases that do not leave the rail straight within a certain margin are eliminated.

Plasticity depth – Rail straightness interpreted alone can be misleading. Since the rail is modeled as initially straight, a load case with unrealistically small loads will pass the straightness criterion since little curvature is ever induced in the simulation. This is remedied by noting the amount of plasticity. The entirety of the head and base yield during the physical straightening process, but the entire section does not go plastic. The simulated load case must meet this condition.

2-D MODEL

With the exception of the ends, every cross-section along the length of the rail experiences the same loading history as it passes through the roller straightener. When the contact forces of the rolls on the rail are ignored, this loading reduces to a time-varying bending moment. The bending moment can be visualized simply as the moment diagram plotted over the length of the rail as in Fig. 3. This time history of the bending moment may be applied to a 2-dimensional model to simulate the roller straightening process. This cross-sectional mesh is representative of every section in the physical rail (except the ends).

The 2-dimensional model treats the roller straightening as a pure bending problem. The direct bearing loads of the rolls on the rail are ignored, which allows the rail cross-section to be represented in two dimensions in a state of generalized plane strain [7]. It is primarily the gross bending of the entire rail section that straightens the rail, so this simplification does not significantly impact the rail curvature predictions for a particular loading scenario. This fact is used to evaluate the plausibility of the candidate load scenarios. The final curvature of the rail is easily determined from a generalized plane strain model (the rotation of the cross-sectional plane is one of the analysis variables), making this model a simple way of evaluating the candidate load cases.

The cross-section is meshed with 1281 quadrilateral elements with bilinear interpolation (designated "CPEG4" elements in ABAQUS). There are 1388 nodes. This mesh is extruded to create the mesh used in the 3-dimensional model described later. The 3-dimensional modeling includes roll-on-rail contact, which in turn controls the element size requirements for the mesh near the surfaces of head and base. These requirements will be discussed in the appropriate section.

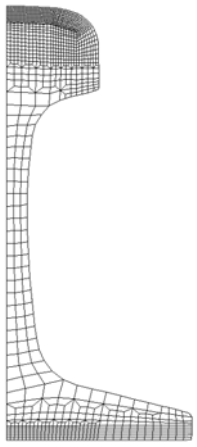

Figure 4. The 2-dimensional GPS mesh.

The rail cross-section is symmetric about the vertical centerline. This symmetry has been exploited in the mesh; only half of the section is included in the model.

The bending moments are applied to the reference node of the cross-section, causing a strain field in the section that varies linearly in the vertical direction. The bending moment at each roll stand is applied and removed linearly across a time step, until the entire sequence is finished. The simulation is executed twice for each of the four load cases, with and without initial heat treatment stresses present.

The maximum final curvature value to judge a load case acceptable is approximately 2×10^{-3} rad/m. This curvature would cause a 24 m length of rail to have a vertical deviation of approximately 12.5 cm at the center of the length (see Fig. 5).

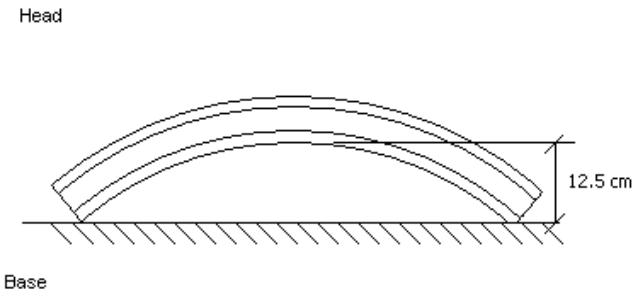

Figure 5. Schematic of a rail at the maximum acceptable curvature.

The curvature of rail section is plotted over the course of the simulation for each load case in Fig. 6. Load case 4 clearly violates the straightness criterion and is therefore judged to be outside of the range of acceptable roller straightening loads. All other load cases meet the straightness requirement.

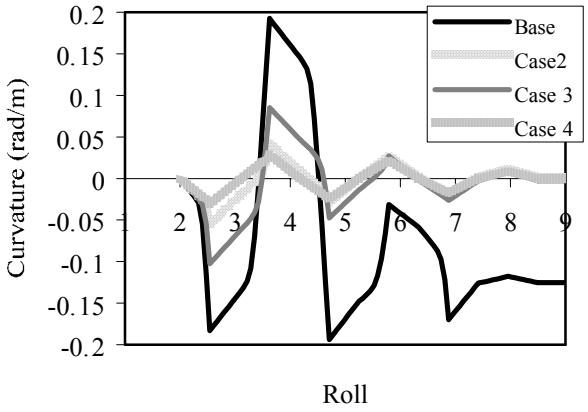

Figure 6. Curvature of the rail during straightening.

The next step is to measure the maximum depth of the elastic-plastic interface (see Fig. 7). In case 4, nearly the entire section deforms plastically. This is an unrealistic result for a finishing process such as roller-straightening. In case 3, virtually no yielding occurs in the rail base. The bending moment is not large enough to induce plastic deformation there. It is probably not possible to straighten the entire rail without permanently deforming both the head and the base. Cases 3 and 4 therefore fall outside the realm of plausible straightening scenarios. Load cases 1 and 2 however, are worthy of further consideration.

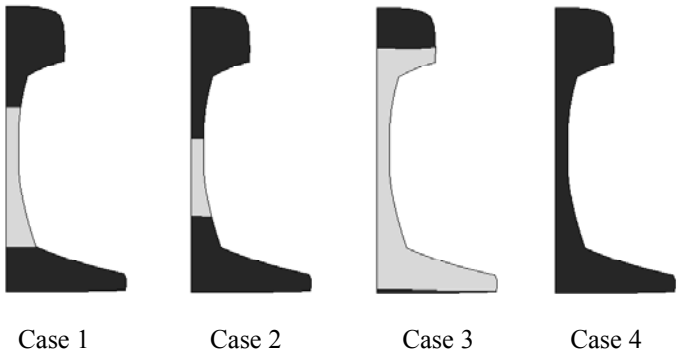

Figure 7. Maximum plastic zone depth. The dark regions are yielding.

The longitudinal residual stress profiles at the end of the roller straightening simulations are shown below in Fig. 8 for load cases 1 and 2. The stress is plotted at the vertical centerline of the rail using element values extrapolated to the nodes and averaged. All stress line plots are presented in this manner. Both plots are typical of residual flexural stresses in beams that are cyclically loaded to cause plastic deformation. The "Z" appearance is a consequence of the application of large, reversed loads. There are 6 bending moment reversals in the roller straightening process. Only 4 produce inelastic behavior in case 1 (see Table 1). There are 5 such bending reversals in case 2. This feature causes the profiles to have similar shapes but opposite signs. The curves intersect at the values of zero stress. Case 2 has larger peak stress values since it contains larger loads than case 1.

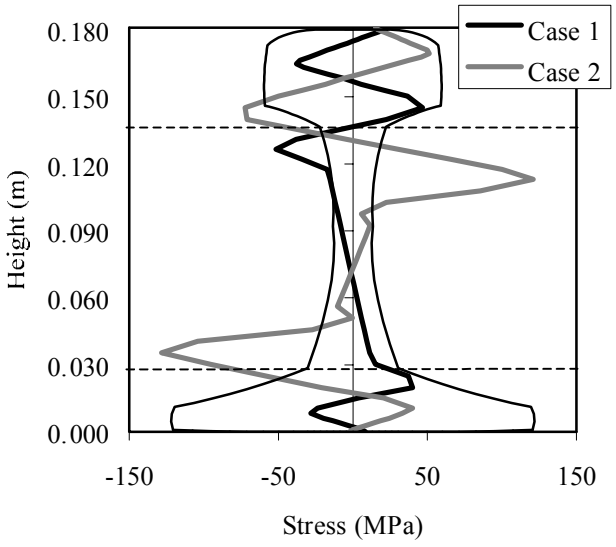

Figure 8. GPS longitudinal residual stress results for Cases 1 and 2.

3-D MODEL

It is necessary to include the roll-on-rail contact in the simulation to discern its influence on the residual stress. The stress field associated with direct bearing problems of this type is 3-dimensional; consequently any finite element model seeking to study these effects will necessarily be 3-dimensional as well. In this section, such a model is described.

The approach taken here is to simplify the problem so that the entire 24 m length of rail is not meshed. The goal is to apply statically equivalent loading on a segment of rail to reproduce the bending and contact load history on a target section. In the roller-straightener, bending moments are applied to the rail by groups of three successive rolls, which will be called "triads". Fig. 9 shows two of these roll triads. Bearing loads exist at every roll stand except the first, leaving six triads in the loading sequence. This loading can be applied one triad at a time to a model.

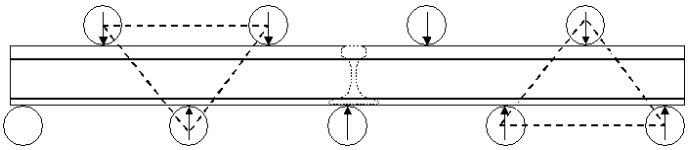

Figure 9. Two roll triads exerting roll forces and bending moments on the rail.

A schematic of the model is depicted in Fig. 10. For each of the six roll triad cycles, there is a target moment, M, and a target roll force, P, to reproduce. In this model, this is accomplished as follows:

The model consists of a short length of rail (less than 1.5 m) with a rigid roller located below the center of the rail as in Fig. 10. To impart the contact force P, two concentrated loads are applied, each with a magnitude $P/2$. Hence, the reaction force developed at the roller will be the target load, P. To simultaneously enforce the correct moment value M, the concentrated loads are applied symmetrically at a distance $2M/P$. In this manner, the section at the center of the mesh is subjected to the same moment and contact forces as the rail in the straightening machine. This stress field at this section then represents at the stress field of the entire physical straightened rail.

This process is repeated for each of the six roll triads. Note that there are actually rollers located both above and below the rail mesh in the model, since the sense of the contact forces and the bending moment alternate at successive roll stands.

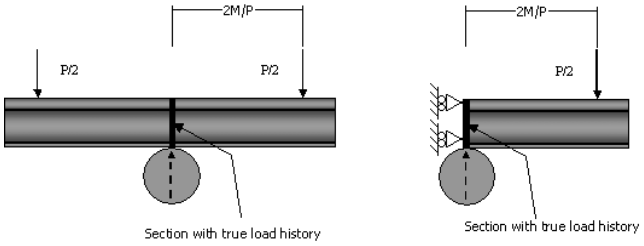

Figure 10. Schematic of the model arrangement.

Symmetry is again utilized to omit half of the rail cross-section. The designed loading scheme also possesses symmetry about the center of the rail span, as shown in Fig. 10. In this manner, only half of the model described above must be meshed.

The rail was discretized using first-order hexahedral continuum elements (designated "C3D8" elements in ABAQUS). Figure 12 shows the mesh generated for this analysis. The model contains 15,683 elements and 35,830 nodes.

The mesh takes advantage of the capability in ABAQUS to "tie" or kinematically couple dissimilar meshes. The degrees of freedom of two meshes can be forced to be the same at a common surface. This allows the meshing of a single domain with multiple groups of elements that do not have nodal connectivity [7]. The technique allows for rapid changes in element density by eliminating transition elements. The portion of the rail mesh in contact with the rolls is more refined, and is tied to a coarser region where the concentrated loads are applied.

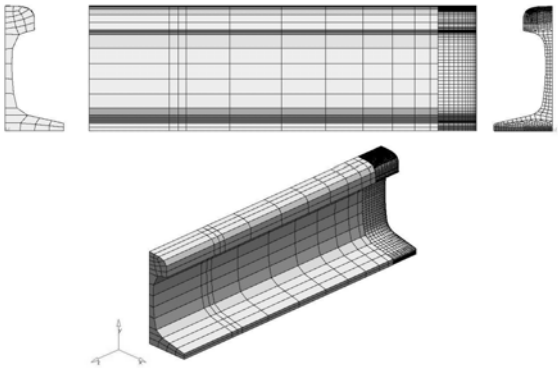

Figure 11. The 3-dimensional mesh.

The rollers are modeled as mathematically defined rigid surfaces (their coarsely discretized appearance in Figure 12 is an artifact of the post-processing software). The top roller conforms to the crown radius of the rail; the bottom roller is cylindrical.

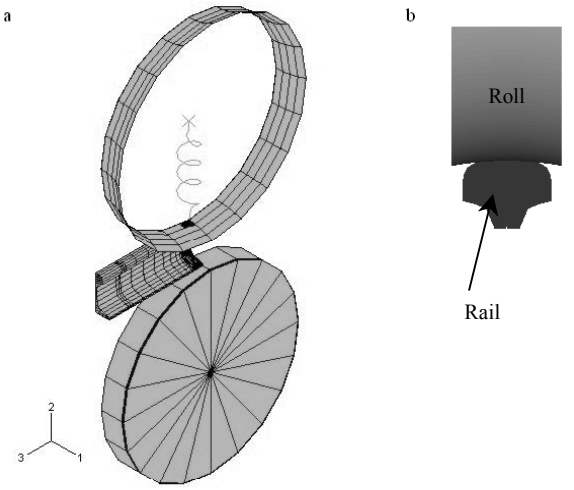

Figure 12. a) Isometric view of model with top and bottom roller. b) Schematic showing the shape of the roller surface.

RESULTS

The 3-dimensional results for load case 1 are similar to the corresponding 2-dimensional ones. The longitudinal residual stress is plotted in Fig. 13, along with the GPS predictions for comparison. Although the roll-on-rail contact alters the stress field, the jagged features of the bending stresses are still recognizable. The contact stress has only a mild impact on the longitudinal stress, especially in the head.

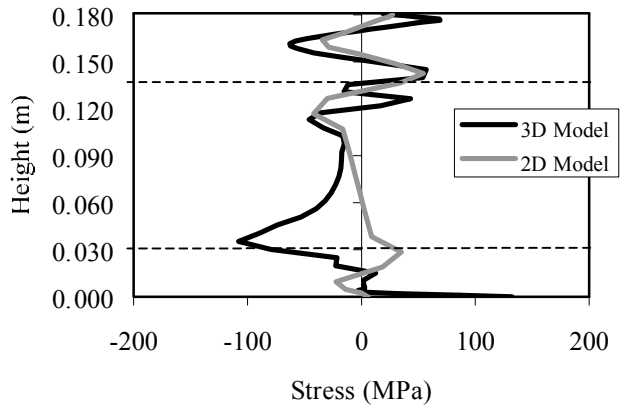

Figure 13. Comparison of the 2-D and 3-D longitudinal residual stress profiles for load case 1.

The 3-dimensional results for load case 3 show a clear difference from the corresponding GPS calculations. The longitudinal stress profiles displayed in Fig. 14 compare the 2-dimensional and 3-dimensional calculations. The inclusion of the contact effects disturbs the stress profile, particularly in the rail web. The stress in the head is much less affected.

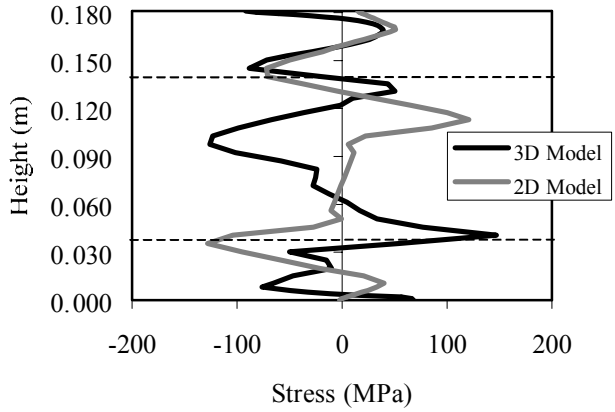

Figure 14. Comparison of the 2-D and 3-D longitudinal residual stress profiles for load case 2.

Figure 15 illustrates how the residual stress distribution evolves in load case 2. The sequence of plots in Fig. 15 compare the calculated longitudinal residual stress of both models after the bending reversal of each roll triad. The loads in this scenario are large enough to show the influence of contact stresses when they do not dominate the bending effects. After the third cycle, two peaks in the web stress (one compressive and one tensile) arise in the 3-dimensional simulation. These features persist to the final distribution. Both 3-dimensional model longitudinal stress results have distinct peaks at the transitions from the head to the web and from the web to the base. The contact stresses increase the peak values of the longitudinal stress at the surfaces of the rail.

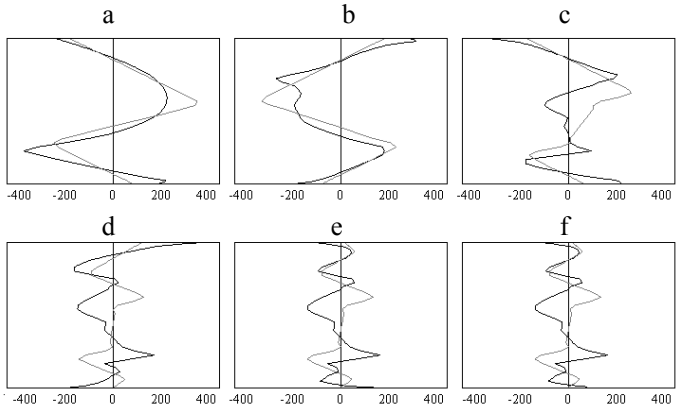

Figure 15 Roll-by-roll comparison of longitudinal stresses in 2-dimensional and 3-dimensional models for case 2. 2-D results are gray lines; 3-D results are black lines.

To examine the effects of rail heat treatment on the roller straightening stresses, simulations are carried out with an initial stress field. The head-hardening heat treatment stresses calculated by R. Fata [2] are used as an initial distribution prior to the roller straightening simulation. The resulting longitudinal stress profile for load case 1 is shown in Fig. 16. The original untreated results and the initial longitudinal stresses are plotted for comparison. Through the head and web, there is a positive shift in the stresses; the longitudinal stress in the base is completely unaffected. Load case 2 displays similar behavior.

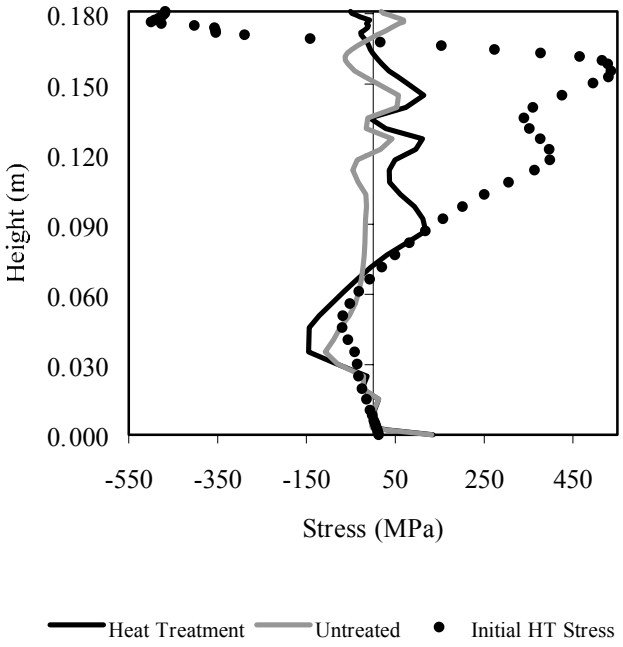

Figure 16. Heat treatment stresses for load case 1.

DISCUSSION AND CONCLUSIONS

Comparison of the 2- and 3-dimensional residual stress results reveals that the magnitude of the contact loads is a decisive influence on the stress field. In particular, the flexural stresses in load case 2 are significantly disturbed by the contact stress, even in portions of the rail web located far from the contact interface. When the contact loads are very high, the stresses are redistributed throughout the section. Therefore it is critical to obtain accurate estimates of the straightening loads to make accurate roller straightening residual stress estimates.

Experimental analyses of the longitudinal stresses in roller-straightened rail must be interpreted carefully. The stress curves presented in the previous section are complex, containing many inflection points and local extrema that would not be characterized well by taking only a few data points. Figure 17 illustrates how a specific sampling distribution could produce a misleading plot from the case 1 longitudinal stress results. Strain gauge measurements taken at the surface of the rail at these points would not resolve the true character of the stress profile.

Neutron diffraction analysis of the residual stresses in rails, including as-manufactured roller-straightened rails, was performed in tandem with these numerical simulations by the National Institute of Standards and Technology in Gaithersburg, MD. These results are presented in a companion paper at this conference.

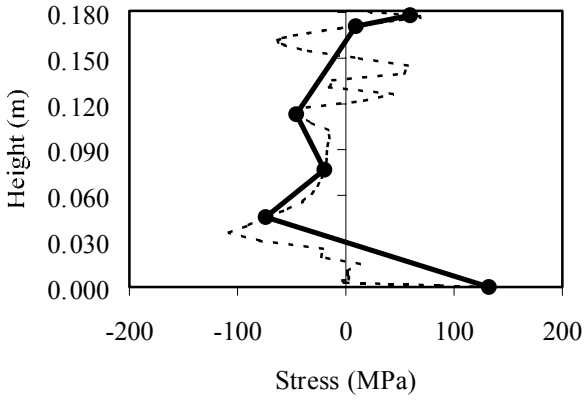

Figure 17 Longitudinal stress profile created by sampling of case 1.

Heat treatment of the rail primarily affects the longitudinal residual stress in the web.

To further study of roller straightening stresses in rail, the sensitivity of the residual stress estimates to material behavior should be investigated. In addition, the non-uniform microstructure due to the heat treatment causes variation in the material properties, which should be taken into account. More complex material behavior, such as nonlinear hardening, remains a consideration for further investigation.

ACKNOWLEDGEMENT

The work was performed by the Volpe National Transportation Systems Center (Volpe Center), in support of the Federal Railroad Administration's (FRA) Track Systems Safety Program, under the direction of Dr. Magdy El-Sibaie, Chief, Track Research Division. Mr. Leonard W. Allen is the Project Manager for the research related to rail integrity.

REFERENCES

[1] J.E. Gordon and A.B. Perlman. "Application of the Constrained Minimization Method to the Prediction of Residual Stresses in Actual Rail Sections", in *Residual Stresses in Rails – Effects on Rail Integrity*

and Railroad Economics. Kluwer Academic Publishers, Dordrecht, the Netherlands. 1992. pp. 151-177.

[2] R.G. Fata. *Residual Stresses Resulting from Quench Hardening the Head of a Railroad Rail.* Master's Thesis, Tufts University, May 1996.

[3] S.J. Wineman. *Residual Stresses and Web Fracture in Roller-Straightened Rail.* Ph.D. Thesis. Massachusetts Institute of Technology, June 1991.

[4] B.E.Varney and T.N. Farris. *Mechanics of Roller Straightening.*

[5] G. Schleinzer and F.D. Fischer. "Residual Stresses in Roller Straightened Rails", in *Proceedings of the Fifth European Conference on Residual Stress, Materials Science Forum*, (A.J. Böttger, R. Delhez, and E.J. Mittemeijer, eds.). Vols. 347-349, 2000. pp. 369-373.

[6] J.W. Ringsberg and T. Lindbäck. "Rolling Contact Fatigue Analysis of Rails Including Numerical Simulations of the Rail Manufacturing Process and Repeated Wheel-Rail Contact Loads", in International *Journal of Fatigue,* 25, 2003. pp. 547-558.

[7] ABAQUS/Standard User's Manual (version 6.4-1). ABAQUS, Inc., Warwick, RI, 2003.

[8] "Model Calculation Relating to the Occurrence of Residual Stresses During Roller-Straightening of Rails", in *Possibilities of Improving the Service Characteristics of Rails by Metallurgical Means, Report No. 4.* Report to Office of Research and Experiments of the International Union of Railways (ORE/UIC), Utrecht, 1987.

[9] B. Talamini. *Residual Stresses in Roller-Straightened Rail.* Master's Thesis, Tufts University, February, 2004.

APPENDIX

Material properties for the heat treatment and roller straightening stress analyses are given in the tables that follow. The elastic modulus is designated E, Poisson's ratio is ν, the yield strength is S_y, the plastic modulus is E_p, and the coefficient of thermal expansion is α. For the roller straightening analysis, room temperature values for all properties are assumed.

Table 3 Mechanical properties of the rail steel.

Temperature (°C)	E (GPa)	ν	S_y (MPa)	E_p (GPa)
24	206.9	0.295	483.0	22.7
230	195.2	0.307	485.1	26.9
358	187.4	0.314	418.8	21.3
452	167.0	0.320	332.4	15.6
567	99.1	0.326	151.1	6.2
704	48.6	0.334	45.0	1.0
900	41.8	0.345	13.4	0.1

Table 4. Coefficient of thermal expansion of the rail steel.

Temperature (°C)	α $\times 10^{-6}$
20	9.7
268	11.0
400	11.7
500	12.2
700	13.2
800	14.0
1040	16.0